Chapter 2

Basic elastodynamic theory

In this chapter the elastodynamic equations describing the propagation of waves in elastic media are presented. Only non-piezoelectric media are considered, i.e. no electric forces are present in the media. The development of the elastodynamic equations involves the important concepts of the stress - and strain tensor, why these are presented in the first two sections. The elastic properties of a material may conveniently be described through the so-called matrix notation, which will be given some attention later in the chapter. With the matrix notation introduced, the crystal systems considered in this thesis are then presented. The chapter ends with a review of existing techniques for solving the elastodynamic equations as well as a description and motivation of the method adopted in this thesis. Much of the basic elastodynamic theory presented here is inspired by classical textbooks on the subject e.g. [2, 7, 42, 68].

2.1 Stress tensor

When a solid body is subjected to a deformation, *internal stresses* (forces per unit area) are introduced attempting to return the body to its original state of equilibrium. In order to characterize these internal stresses, we consider a rectangular coordinate system with orthogonal unit vectors $\boldsymbol{e}_1$, $\boldsymbol{e}_2$, $\boldsymbol{e}_3$.

At an arbitrary point P in the body we consider the stress vector (or traction vector) $\boldsymbol{t}^{(\boldsymbol{e}_1)}$ acting on a surface with surface normal $\boldsymbol{e}_1$. The stress vector can be resolved into components σ_{i1} along the three base vectors $\boldsymbol{e}_i$ as

$$\sigma_{i1} = \boldsymbol{t}^{(\boldsymbol{e}_1)} \cdot \boldsymbol{e}_i, \qquad i = 1, 2, 3$$

Here we employ the convention, that the stress vector (and therefore the stress components) denotes the stress exerted by the material on the positive side of the surface (the direction of the chosen normal vector) on the material on the other (negative) side of the surface. By Newton's third law, the material on the negative side of the surface exerts a stress on the material on the positive side of the surface equal in size and opposite in direction. In a similar way we define the components σ_{i2} and σ_{i3} ($i = 1, 2, 3$) by considering stress vectors $\boldsymbol{t}^{(\boldsymbol{e}_2)}$ and $\boldsymbol{t}^{(\boldsymbol{e}_3)}$ acting on surfaces through P with surface normals $\boldsymbol{e}_2$ and $\boldsymbol{e}_3$ respectively. From the knowledge of the nine components σ_{ij}, the stress vector $\boldsymbol{t}^{(\boldsymbol{n})}$ acting on an arbitrary surface through P with surface normal $\boldsymbol{n}$ can be calculated as [58]

$$t_j^{(\boldsymbol{n})} = n_i \sigma_{ij} \qquad (2.1)$$

$\boldsymbol{t}^{(\boldsymbol{n})}$ and $\boldsymbol{n}$ being first order tensors and linearly related through σ_{ij} by (2.1) implies that σ_{ij} form a second order tensor [58] called the *stress tensor*. The diagonal elements of the tensor are called normal components while the off-diagonal elements are called shear components. In the special case where the stress tensor is independent of position, it is called *homogeneous*. However, in general the stress tensor depends on position (and time) $\sigma_{ij} = \sigma_{ij}(\boldsymbol{x}, t)$, in which case it is called *inhomogeneous*. In the absence of body torques the important result can be shown [7] that the stress tensor is symmetric[1]

$$\sigma_{ij} = \sigma_{ji} \tag{2.2}$$

This property is fundamental to the development of the elastodynamic equations in section 2.3.

2.2 Strain tensor

During the deformation of a body, a point initially at position $\boldsymbol{x}$ is displaced to a new position $\boldsymbol{x}' = \boldsymbol{x} + \boldsymbol{u}$, where $\boldsymbol{u} = \boldsymbol{u}(\boldsymbol{x}, t)$ denotes the *displacement vector* characterizing the deformation of the body. Consider now two points close together connected through the radius vector $\mathrm{d}\boldsymbol{x}$, the squared length of which is $\mathrm{d}l^2 = \mathrm{d}x_k^2$. After the deformation, a new radius vector $\mathrm{d}\boldsymbol{x}' = \mathrm{d}\boldsymbol{x} + \mathrm{d}\boldsymbol{u}$ with the squared length $\mathrm{d}l'^2 = \mathrm{d}x_k'^2 = (\mathrm{d}x_k + \mathrm{d}u_k)^2$ is joining the two displaced points. Substituting $\mathrm{d}u_k = u_{k,l}\mathrm{d}x_l$ we obtain

$$\mathrm{d}l'^2 = \mathrm{d}l^2 + 2\epsilon_{kl}\mathrm{d}x_k\mathrm{d}x_l$$

where

$$\epsilon_{kl} = \frac{1}{2}(u_{k,l} + u_{l,k} + u_{j,k}u_{j,l}) \tag{2.3}$$

is called the *strain tensor*, which is immediately seen to be symmetric. From the above equations, it is seen that the strain tensor is an expression for the relative deformation at a point. That (2.3) indeed defines a tensor is a basic fact shown in most textbooks on the subject, e.g. [58]. In this thesis we consider small deformations only for which the last second order term in u_j can be neglected. Thus, here we consider the strain tensor[2]

$$\epsilon_{kl} = \frac{1}{2}(u_{k,l} + u_{l,k}) \tag{2.4}$$

The diagonal elements of the strain tensor $\epsilon_{ii} = u_{i,i}$ (no summation) are called tensile strains or stretches. These elements describe the relative elongation of a small volume (Fig. 2.1) along the three coordinate axes. As a consequence, the change in volume of the unit cube is given by $(1+\epsilon_{11})(1+\epsilon_{22})(1+\epsilon_{33}) - 1 \approx \epsilon_{ii}$ for small strains, i.e. the trace of the strain tensor. The off-diagonal elements are called shear strains. They describe the relative shearing perpendicular to the coordinate axes of opposite faces of the volume and are not associated with any change of volume.

[1]However, even in the case of body torques present (e.g. due to polarization or magnetization), the stress tensor can be considered symmetric [58] if the stress tensor is redefined as its symmetrical part $\frac{1}{2}(\sigma_{ij} + \sigma_{ji})$ in Hooke's law (2.5).

[2]It may be noted that (2.4) defines a satisfactory measure of the deformation as it is zero for pure translations or rotations of the medium. These are not considered true deformations of the medium.

2.3 Elastodynamic equations

Internal stresses σ_{ij} present in a medium result in finite strains ϵ_{kl}. This basic observation can be regarded as a functional dependence between the two tensors i.e. $\epsilon_{kl} = \epsilon_{kl}(\sigma_{ij})$. We may also consider the inverse functional dependence $\sigma_{ij} = \sigma_{ij}(\epsilon_{kl})$. These relationships to first order are known as (the generalized) Hooke's law

$$\sigma_{ij} = c_{ijkl}\epsilon_{kl} \tag{2.5}$$
$$\epsilon_{kl} = s_{klij}\sigma_{ij} \tag{2.6}$$

generalizing the basic (empirical) formula for a long thin rod involving Young's module. c_{ijkl} is known as the fourth-order *elastic stiffness tensor* while s_{klij} denotes the fourth-order *elastic compliance tensor*, both containing $3^4 = 81$ components. That c_{ijkl} and s_{klij} are in fact fourth-order tensors follows immediately from the fact that they linearly relate two second-order tensors.

The stress tensor and strain tensor both being symmetric provides us with a certain degree of freedom in choosing the components of the two fourth-order tensors[3] c_{ijkl} and s_{klij}. As a result we may impose the following pairwise symmetry properties on their subscripts

$$c_{ijkl} = c_{jikl} = c_{ijlk} \tag{2.7}$$
$$s_{ijkl} = s_{jikl} = s_{ijlk} \tag{2.8}$$

This reduces the number of independent components from 81 to $6^2 = 36$ components for both tensors. Using (2.7) together with (2.4), we may write Hooke's law in the form

$$\sigma_{ij} = c_{ijkl}u_{k,l} \tag{2.9}$$

relating the stress tensor and the displacement vector.

Having introduced Hooke's law in the form (2.9), this paragraph is devoted to the presentation of the equations of motion for the three components of the displacement vector. As an example, the equation of motion for u_1 is derived with reference to the small cube in Fig. 2.1. The cube is positioned with one of its corners at $P = (x_1, x_2, x_3)$ and with dimensions $\mathsf{d}x_1$, $\mathsf{d}x_2$, $\mathsf{d}x_3$. The total force acting on the cube in the $\boldsymbol{e}_1$ direction equals the sum of forces in that direction exerted by the surroundings on the cube across each surface plus the contribution from a body force if present. The occurrence of a minus is due to the definition of the stress tensor as discussed in section 2.1. We then obtain, setting $\mathsf{d}V = \mathsf{d}x_1\mathsf{d}x_2\mathsf{d}x_3$

$$\begin{aligned}\rho\ddot{u}_1\mathsf{d}V &= [-\sigma_{11}(x_1) + \sigma_{11}(x_1 + \mathsf{d}x_1)]\mathsf{d}x_2\mathsf{d}x_3 + \\ &\quad [-\sigma_{12}(x_2) + \sigma_{12}(x_2 + \mathsf{d}x_2)]\mathsf{d}x_1\mathsf{d}x_3 + \\ &\quad [-\sigma_{13}(x_3) + \sigma_{13}(x_3 + \mathsf{d}x_3)]\mathsf{d}x_1\mathsf{d}x_2 + \\ &\quad \mathsf{d}V\rho f_1\end{aligned}$$

where ρ is the mass density and f_1 denotes the force per unit mass in the $\boldsymbol{e}_1$ direction.

[3] In the sense that in an experiment certain components of the two tensors cannot be determined separately whereas their sum can.

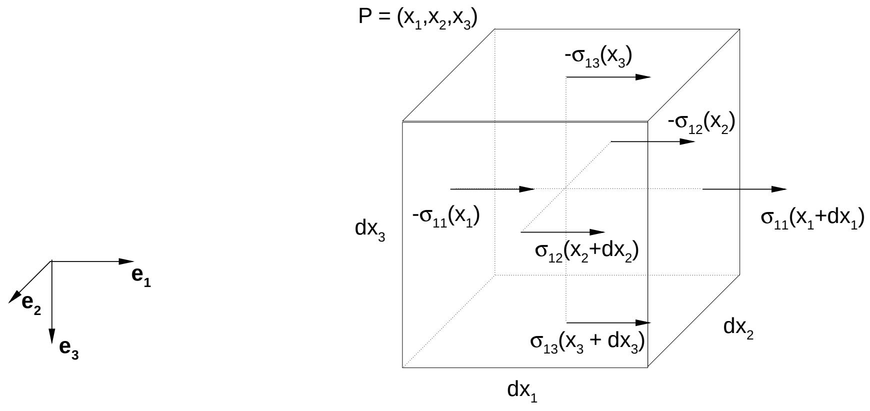

Figure 2.1: Stress components acting on a small cube and influencing the motion of u_1.

Substituting $\sigma_{1j}(x_j+\mathrm{d}x_j) \approx \sigma_{1j}(x_j)+\sigma_{1j,j}(x_j)\mathrm{d}x_j$ (no summation) and removing canceling terms, we obtain the equation of motion for the u_1 component

$$\rho\ddot{u}_1 = \sigma_{1j,j} + \rho f_1$$

In a similar way, the equation of motion may be obtained for the other two components, thus obtaining the equations of motion with f_i denoting force per unit mass in direction $\boldsymbol{e}_i$

$$\rho\ddot{u}_i = \sigma_{ij,j} + \rho f_i \tag{2.10}$$

An example of a body force could be a point force inside the medium. This problem has received a lot of attention within the area of analytic modelling e.g. [71]. The gravitational force is usually neglected as will be the case in this thesis. (2.9) together with (2.10) describe the dynamic deformation of a solid body subjected to applied forces. In the case where the elastic stiffness tensor is constant (2.9) is often inserted into (2.10) to yield

$$\rho\ddot{u}_i = c_{ijkl}u_{k,jl} + \rho f_i, \qquad i = 1,2,3 \tag{2.11}$$

resulting in three coupled second order partial differential equations in u_i.

Up to now, the equations governing the wave propagation in elastic media (2.9) and (2.10) have been developed. In order to make the problem mathematically well-defined, initial - and boundary conditions must be specified as well. To this end, we consider a bounded elastic medium B as shown in Fig. 2.2 representing the medium to be inspected. The boundary is denoted by S with the part of the boundary under the transducer denoted by T. As initial condition, it is required that $\boldsymbol{u}(\boldsymbol{x},t) = \boldsymbol{0}$ for $t < 0$ [71, 72]. Concerning the boundary conditions at S, several possibilities exist [2]

1. the displacement vector $\boldsymbol{u}(\boldsymbol{x},t)$ is prescribed at the boundary at all times.
2. the traction vector $t_i(\boldsymbol{x},t) = \sigma_{ij}(\boldsymbol{x},t)n_j$ is prescribed at the boundary at all times.
3. a combination of 1) and 2) at different parts of the boundary (mixed boundary conditions).

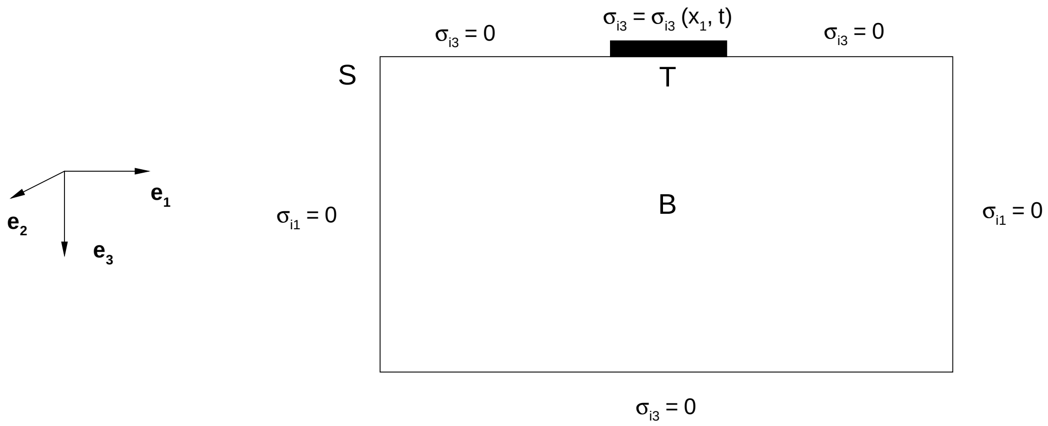

Figure 2.2: Illustration of the considered boundary conditions involving traction vectors.

In the scenarios considered in this thesis resembling actual ultrasonic inspection situations, we shall be concerned exclusively with condition 2 as illustrated in Fig. 2.2. That is, the test specimen is placed in open air (approximated by vacuum) with a boundary free to move. This results in the traction vector being zero at the boundary $\boldsymbol{x} \in S - T$ (a so-called free boundary), while directly under the transducer $\boldsymbol{x} \in T$, the traction vector is prescribed according to the chosen transducer model. In chapter 3 on analytic modelling, the two vertical boundaries as well as the lower horizontal boundary tend to infinity, thus modelling a half-space with one free surface.

The medium is characterized by the mass density ρ and the elastic stiffness tensor c_{ijkl} entering the equations. The medium is called *inhomogeneous*, if one (or both) of these material properties depend upon the position in the medium and *homogeneous* otherwise. This deserves some elaboration. Whereas the word inhomogeneous in certain contexts may be used to make a distinction between materials based on their bulk properties (f. ex. mass density) defining some large-scale material boundaries, we shall here, as stated above, use the word whenever the material properties $\rho(\boldsymbol{x})$ or $c_{ijkl}(\boldsymbol{x})$ depends on the position in the medium. Adopting this attitude is natural from a mathematical point of view, since this is exactly what makes the mathematical problem complex to a smaller or larger extent, no matter whether the involved materials are identical or not. An example illustrating this use of the word is that of the austenitic weld treated in detail in chapter 6. Such a weld is modelled as consisting of grains of the same transversely isotropic weld material (and thus with the same mass density), but with the orientation of the crystal axes of this material changing from grain to grain (and thus with the elastic stiffness tensor c_{ijkl} changing from grain to grain).

At this point it seems appropriate to summarize the elastodynamic problem describing wave propagation in a bounded elastic medium $\mathcal{B}$, this being the main topic of this thesis. If the material is inhomogeneous, the elastodynamic problem may be formulated as in (2.12) below. This is well-suited for a numerical approach, and this is the way the elastodynamic problem will be solved in chapter 4. We set $f_i = 0$ and for simplicity, only the initial condition and boundary condition 2 as described above are included

$$\boxed{\begin{array}{ll} \rho(\boldsymbol{x})\ddot{u}_i(\boldsymbol{x},t) = \sigma_{ij,j}(\boldsymbol{x},t), & i = 1,2,3 \\ \sigma_{ij}(\boldsymbol{x},t) = c_{ijkl}(\boldsymbol{x})u_{k,l}(\boldsymbol{x},t), & i,j = 1,2,3 \\ & \\ \boldsymbol{u}(\boldsymbol{x},t) = \boldsymbol{0}, & t < 0 \\ \boldsymbol{t}(\boldsymbol{x},t) = \left\{ \begin{array}{ll} \boldsymbol{0}, & \boldsymbol{x} \in S - T \\ \boldsymbol{h}(\boldsymbol{x},t), & \boldsymbol{x} \in T \end{array} \right. & \end{array}} \tag{2.12}$$

This formulation of the elastodynamic problem may be reformulated in the so-called matrix notation, see (2.21), in the next section.

In the case of homogeneous media often considered in analytic modelling [71, 72] $c_{ijkl}(\boldsymbol{x}) = c_{ijkl}$ (and $\rho(\boldsymbol{x}) = \rho$), the use of (2.11) may be more convenient[4], and the problem is formulated as in (2.13) below.

$$\boxed{\begin{array}{ll} \rho\ddot{u}_i(\boldsymbol{x},t) = c_{ijkl}u_{k,jl}(\boldsymbol{x},t), & i = 1,2,3 \\ & \\ \boldsymbol{u}(\boldsymbol{x},t) = \boldsymbol{0}, & t < 0 \\ \boldsymbol{t}(\boldsymbol{x},t) = \left\{ \begin{array}{ll} \boldsymbol{0}, & \boldsymbol{x} \in S - T \\ \boldsymbol{h}(\boldsymbol{x},t), & \boldsymbol{x} \in T \end{array} \right. & \end{array}} \tag{2.13}$$

If an isolated inhomogeneity or a material boundary is to be included in this kind of modelling, the boundary conditions at the interfaces must be dealt with explicitly. If a void is modelled, traction free surfaces are usually required. Note, that such a boundary condition also must dealt with explicitly in the approach (2.12). Another typical example is the reflection–refraction problem of plane waves at an interface between two materials. Typically, the boundary conditions require continuous displacement vector and traction vector across the interface. This case is automatically handled in the approach (2.12).

2.4 Matrix notation

In the previous sections, extensive use has been made of tensors and their notation. One of the reasons for working with tensors is the familiar one, that tensors are easily transformed under a change of coordinate system. This is an important property of the elastic stiffness tensor especially when working in inhomogeneous media. However, the underlying mechanisms and physical principles may not always leap to the eye, and the notation may become unnecessary complex especially considering the revealed symmetry properties of the tensors introduced so far. An equivalent matrix notation has therefore been developed for the theory of elasticity based on the following transformation scheme between a pair of tensor subscripts and a single matrix subscript [7, 58]

$$\boxed{\begin{array}{lcccccc} \text{tensor notation} & 11 & 22 & 33 & 23,32 & 31,13 & 12,21 \\ & \updownarrow & \updownarrow & \updownarrow & \updownarrow & \updownarrow & \updownarrow \\ \text{matrix notation} & 1 & 2 & 3 & 4 & 5 & 6 \end{array}} \tag{2.14}$$

[4]This splitting up in (2.12) and (2.13) should not be regarded as a widely agreed pracsis. Rather it reflects the author's impression as well as showing different ways of presenting the problem.

In matrix notation, both the stress tensor and the strain tensor can be written as column vectors. By convention, however, for some of the strain components ($i = 4, 5, 6$), a factor of $\frac{1}{2}$ is introduced. The same symbols are used since no confusion can occur. The two representations are thus related as

$$\begin{pmatrix}\sigma_{11}\\ \sigma_{22}\\ \sigma_{33}\\ \sigma_{23}\\ \sigma_{13}\\ \sigma_{12}\end{pmatrix} \equiv \begin{pmatrix}\sigma_{1}\\ \sigma_{2}\\ \sigma_{3}\\ \sigma_{4}\\ \sigma_{5}\\ \sigma_{6}\end{pmatrix}, \qquad \begin{pmatrix}\epsilon_{11}\\ \epsilon_{22}\\ \epsilon_{33}\\ \epsilon_{23}\\ \epsilon_{13}\\ \epsilon_{12}\end{pmatrix} = \begin{pmatrix}u_{1,1}\\ u_{2,2}\\ u_{3,3}\\ \frac{1}{2}(u_{2,3}+u_{3,2})\\ \frac{1}{2}(u_{1,3}+u_{3,1})\\ \frac{1}{2}(u_{1,2}+u_{2,1})\end{pmatrix} \equiv \begin{pmatrix}\epsilon_{1}\\ \epsilon_{2}\\ \epsilon_{3}\\ \frac{1}{2}\epsilon_{4}\\ \frac{1}{2}\epsilon_{5}\\ \frac{1}{2}\epsilon_{6}\end{pmatrix} \tag{2.15}$$

In matrix notation, the elastic stiffness tensor becomes a 6×6 matrix c_{ij}. It can be shown, e.g. [58], that the work necessary to produce a strain ϵ_j per unit volume, called the strain energy density $\mathcal{E}$, is equal to

$$\mathcal{E} = \frac{1}{2} c_{ij}\epsilon_i\epsilon_j > 0 \tag{2.16}$$

Now, for physical reasons we must require (as indicated) that this expression is non-negative and furthermore that it is zero if and only if $\epsilon_i = 0$, $i = 1, \ldots, 6$. Thus, the matrix c_{ij} must be positive-definite and symmetric

$$c_{ij} = c_{ji} \tag{2.17}$$

This reduces the maximum number of independent elastic constants from 36 to 21. The number of independent constants is usually much smaller for a particular anisotropic material as will be shown in the next section. An additional advantage of working in the matrix notation is, that this representation is often used in scientific papers, text books etc. containing values for elastic constants.

It may easily be shown that (due to the convention of the above introduced factor of $\frac{1}{2}$) Hooke's law (2.9) in matrix notation becomes

$$\sigma_i = c_{ij}\epsilon_j, \qquad i = 1, \ldots, 6 \tag{2.18a}$$

$$\epsilon_i = s_{ij}\sigma_j, \qquad i = 1, \ldots, 6 \tag{2.18b}$$

Thus, we have the important result, that the elastic compliance matrix is simply the inverse of the elastic stiffness matrix

$$\boldsymbol{s} = \boldsymbol{c}^{-1} \tag{2.19}$$

For later use in chapter 4, using (2.18) together with (2.15), Hooke's law in a mixed matrix-tensor notation becomes

$$\begin{pmatrix}\sigma_{11}\\ \sigma_{22}\\ \sigma_{33}\\ \sigma_{23}\\ \sigma_{13}\\ \sigma_{12}\end{pmatrix} = \boldsymbol{c}\begin{pmatrix}\epsilon_{11}\\ \epsilon_{22}\\ \epsilon_{33}\\ 2\epsilon_{23}\\ 2\epsilon_{13}\\ 2\epsilon_{12}\end{pmatrix}, \qquad \begin{pmatrix}\epsilon_{11}\\ \epsilon_{22}\\ \epsilon_{33}\\ 2\epsilon_{23}\\ 2\epsilon_{13}\\ 2\epsilon_{12}\end{pmatrix} = \boldsymbol{s}\begin{pmatrix}\sigma_{11}\\ \sigma_{22}\\ \sigma_{33}\\ \sigma_{23}\\ \sigma_{13}\\ \sigma_{12}\end{pmatrix} \tag{2.20}$$

In the previous section, the elastodynamic problem was formulated in tensor notation (2.12). This problem may conveniently be restated using Hooke's law in the mixed matrix-tensor notation. For the sake of completeness, the full problem statement is repeated

$$\boxed{\begin{array}{l}
\rho(\boldsymbol{x})\ddot{u}_i(\boldsymbol{x},t) = \sigma_{ij,j}(\boldsymbol{x},t), \qquad i = 1,2,3 \\[2ex]
\begin{pmatrix}\sigma_{11}\\ \sigma_{22}\\ \sigma_{33}\\ \sigma_{23}\\ \sigma_{13}\\ \sigma_{12}\end{pmatrix} = \begin{pmatrix} c_{11} & c_{12} & c_{13} & c_{14} & c_{15} & c_{16}\\ c_{12} & c_{22} & c_{23} & c_{24} & c_{25} & c_{26}\\ c_{13} & c_{23} & c_{33} & c_{34} & c_{35} & c_{36}\\ c_{14} & c_{24} & c_{34} & c_{44} & c_{45} & c_{46}\\ c_{15} & c_{25} & c_{35} & c_{45} & c_{55} & c_{56}\\ c_{16} & c_{26} & c_{36} & c_{46} & c_{56} & c_{66}\end{pmatrix} \begin{pmatrix} u_{1,1}\\ u_{2,2}\\ u_{3,3}\\ u_{2,3}+u_{3,2}\\ u_{1,3}+u_{3,1}\\ u_{1,2}+u_{2,1}\end{pmatrix} \\[2ex]
\boldsymbol{u}(\boldsymbol{x},t) = \mathbf{0}, \qquad t < 0 \\
\boldsymbol{t}(\boldsymbol{x},t) = \begin{cases} \mathbf{0}, & \boldsymbol{x} \in S - T \\ \boldsymbol{h}(\boldsymbol{x},t), & \boldsymbol{x} \in T \end{cases}
\end{array}} \tag{2.21}$$

where the elastic matrix has been written in its most general symmetric form. Using this formulation, the elastodynamic equations may straightforwardly be written out in full for a given elastic matrix. Elastic matrices used in this thesis are the topic of the next section.

It should be emphasized that the elastic matrix (as well as the stress and strain column vectors) introduced in this section are not tensors and therefore do not transform as such under a coordinate rotation. Perhaps the biggest single reason for the success of the matrix notation is nevertheless the ease, despite this fact, with which the elastic matrix can be transformed under a coordinate rotation. This result which is due to the work of Bond [11] is recapitulated in the following.

As described later, crystals may be divided into one of seven crystal systems based on their elastic symmetry properties. For each crystal system a set of three mutually orthogonal axes, called the crystal coordinate system, have been defined according to some established practice [58]. It is with respect to these axes, that values for elastic constants are given in tables. Typically, it is desirable to know these values in some fixed laboratory system. To this end, the *Euler angles* (ϕ, θ, ψ) are introduced. The angle ϕ describes the rotation of the crystal coordinate system around the x_3-axis of the laboratory system, θ the rotation of the crystal coordinate system around the x_2-axis and finally ψ the rotation of the crystal coordinate system around the x_3-axis again. An arbitrary rotation[5] of the crystal may be specified through these three angles [7]. However, first we start out with the standard rotation matrix containing the direction cosines

$$\begin{pmatrix} a_{11} & a_{12} & a_{13}\\ a_{21} & a_{22} & a_{23}\\ a_{31} & a_{32} & a_{33}\end{pmatrix}$$

where a_{ij} is the cosine to the angle between the i'th laboratory coordinate axis and the j'th crystal coordinate axis. Inserting this into the transformation law for fourth-order tensors (see e.g. [58])

$$\bar{c}_{ijkl} = a_{im}a_{jn}a_{kp}a_{lq}c_{mnpq}$$

[5]A rotation θ around the x_1-axis is given by $(\phi,\theta,\psi) = (\frac{\pi}{2},\theta,-\frac{\pi}{2})$.

and utilizing the matrix notation introduced earlier one ends up with the following transformation law for the elastic matrix

$$\boldsymbol{c}' = \boldsymbol{M}\boldsymbol{c}\boldsymbol{M}^T \tag{2.22}$$

where the general expression for the 6×6 matrix $\boldsymbol{M}$ is given by (A.1). Since the Euler angles describe an arbitrary rotation, the matrix $\boldsymbol{M}$ may be considered a function of these, $\boldsymbol{M} = \boldsymbol{M}(\phi, \theta, \psi)$. As an example, for a rotation around the laboratory x_2-axis, we have

$$\boldsymbol{M}(0,\theta,0) = \begin{pmatrix} \cos^2(\theta) & 0 & \sin^2(\theta) & 0 & \sin(2\theta) & 0 \\ 0 & 1 & 0 & 0 & 0 & 0 \\ \sin^2(\theta) & 0 & \cos^2(\theta) & 0 & -\sin(2\theta) & 0 \\ 0 & 0 & 0 & \cos(\theta) & 0 & -\sin(\theta) \\ -\frac{\sin(2\theta)}{2} & 0 & \frac{\sin(2\theta)}{2} & 0 & \cos(2\theta) & 0 \\ 0 & 0 & 0 & \sin(\theta) & 0 & \cos(\theta) \end{pmatrix} \tag{2.23}$$

with rotations around the x-axis and z-axis given by (A.2) and (A.4) respectively. (2.22) is a very important result when working in anisotropic, inhomogeneous materials and it will be used extensively in later chapters.

2.5 Crystal systems and their elastic matrices

In the last section, the 6×6 elastic matrix $\boldsymbol{c}$ was introduced and it was shown that it must be symmetric giving a maximum of 21 independent components. Due to this symmetry property, all elastic matrices in this thesis are written showing only the upper triangular part. Thus, the elastic matrix in its most general form can be written

$$\boldsymbol{c} = \begin{pmatrix} c_{11} & c_{12} & c_{13} & c_{14} & c_{15} & c_{16} \\ & c_{22} & c_{23} & c_{24} & c_{25} & c_{26} \\ & & c_{33} & c_{34} & c_{35} & c_{36} \\ & & & c_{44} & c_{45} & c_{46} \\ & & & & c_{55} & c_{56} \\ & & & & & c_{66} \end{pmatrix} \tag{2.24}$$

As mentioned earlier, crystals can be divided into seven crystal systems based on their physical symmetry properties. It is mentioned in passing, that the system with no symmetry properties is called *triclinic* and the corresponding matrix is given by (2.24).

In the following subsections, the three crystal systems considered in this thesis together with their corresponding elastic matrices will be presented. The appearance of a particular elastic matrix can often be deduced from physical symmetry arguments. However, perhaps a more straightforward approach is the combination of the elastic matrix rotation (2.22) with the symmetry properties for the particular crystal system applied to the resulting rotated elastic matrix. The latter approach will be taken here. Zero elements are denoted by a small dot $(\cdot)$. The number of independent elastic constants is in each case shown as a subscript to the matrix.

2.5.1 Isotropic material

A material exhibiting isotropy, being a macroscopic property rather than a crystal property, is elastically identical in all directions. This implies, that the elastic matrix should be invariant under all rotations with respect to any direction in (2.22). This results in the following elastic matrix with two independent constants

$$\boldsymbol{c} = \begin{pmatrix} c_{11} & c_{12} & c_{12} & \cdot & \cdot & \cdot \\ & c_{11} & c_{12} & \cdot & \cdot & \cdot \\ & & c_{11} & \cdot & \cdot & \cdot \\ & & & c_{44} & \cdot & \cdot \\ & & & & c_{44} & \cdot \\ & & & & & c_{44} \end{pmatrix}_{(2)}, \qquad c_{12} = c_{11} - 2c_{44} \tag{2.25}$$

In the isotropic case, the elastic properties are often expressed in terms of the Lamé constants λ and μ (shear modulus) with the relations

$$c_{11} = \lambda + 2\mu \tag{2.26a}$$

$$c_{12} = \lambda \tag{2.26b}$$

$$c_{44} = \mu \tag{2.26c}$$

Using (2.25) together with (2.21) the well-known coupled elastodynamic equations expressed with Lamé constants are easily derived

$$\rho \ddot{u}_i = (\lambda + \mu) u_{k,ki} + \mu u_{i,kk}, \qquad i = 1, 2, 3 \tag{2.27}$$

Often, in an analytic approach, the coupling between the equations (2.27) is removed by using the Helmholtz decomposition of the deformation vector into the gradient of a scalar and the curl of a vector, $\boldsymbol{u} = \nabla\varphi + \nabla \times \boldsymbol{\psi}$ (no connection to Euler angles). Substitution of this decomposition into (2.27) leads to a set of uncoupled wave equations in φ and $\boldsymbol{\psi}$ [2]. Unfortunately, this new set of equations may again be coupled through boundary conditions.

Within ultrasonic, macroscopically isotropic steel components are typically encountered. Table 2.1 shows the elastic constants for typical steel components together with the sound velocities.

Name		Ferritic steel	Austenitic steel
ρ	$[10^3 \mathrm{kg/m^3}]$	7.9	8.42
c_{11}	$[10^{11} \frac{N}{m^2}]$	2.750	2.792
c_{12}		1.132	1.140
v_l	$[\frac{m}{s}]$	5900	5758
v_t		3200	3132

Table 2.1: Elastic properties for typical isotropic steel components.

2.5.2 Cubic crystal

The symmetry of a cubic crystal, characteristic of metals, is the result of three orthogonal 2-fold[6] axes as well as a 3-fold body diagonal in the cube made up of the orthogonal axes.

[6]An axis is called an n-fold axis if the crystal is invariant under a rotation around the axis through the angle $360°/n$.

The latter makes the three 2-fold axes elastically equivalent. The three 2-fold axes are arranged such that they are parallel to the crystal coordinate axes. They imply a matrix on the form (2.25). However, the 3-fold axis puts less constraints on the constants resulting in the following elastic matrix containing three independent elastic constants

$$\boldsymbol{c} = \begin{pmatrix} c_{11} & c_{12} & c_{12} & \cdot & \cdot & \cdot \\ & c_{11} & c_{12} & \cdot & \cdot & \cdot \\ & & c_{11} & \cdot & \cdot & \cdot \\ & & & c_{44} & \cdot & \cdot \\ & & & & c_{44} & \cdot \\ & & & & & c_{44} \end{pmatrix}_{(3)} \tag{2.28}$$

Obviously, the cubic elastic matrix differ from the isotropic elastic matrix only in c_{44}, which may be chosen arbitrarily in the cubic case, but is given by the expression $\frac{1}{2}(c_{11} - c_{12})$ in the isotropic case (2.25). As a measure of the anisotropy, one therefore often talks about the anisotropy factor A [40] for cubic media defined as the ratio[7]

$$A = \frac{2c_{44}}{c_{11} - c_{12}} \tag{2.29}$$

Often used weld metals are austenitic steel X 6 CrNi 18 12 [14,48] and Inconel 182. The single crystal cubic elastic constants for these two metals together with their anisotropic factors are given in Table 2.2. It has not been possible to obtain elastic constants directly for Inconel 182. Values for similar metals have been obtained and from these a suitable set has been chosen, see f. ex. [5] and references therein. As seen, the anisotropic factor is somewhat higher (a factor 2) for austenitic steel.

Name		X 6 CrNi 18 12	Inconel 182
ρ	$[10^3 \mathrm{kg/m^3}]$	7.90	8.606
c_{11}	$[10^{11}\frac{N}{m^2}]$	2.16	2.5376
c_{12}		1.45	1.3889
c_{44}		1.29	1.06
A		3.63	1.85

Table 2.2: Cubic elastic properties and anisotropic factor (2.29) of typical weld metals.

2.5.3 Transversely isotropic crystal

In a transversely isotropic (hexagonal) crystal there exists exactly one plane in which the elastic properties are the same in all directions. The axis normal to this plane is called the symmetry axis and is usually taken to be parallel to the z-axis[8] of the crystal coordinate system. The corresponding general elastic matrix is deduced from (2.24) by demanding that the elastic matrix $\boldsymbol{c}$ should be invariant under an arbitrary rotation ϕ with respect to the x_3-axis, that is from (2.22)

$$\boldsymbol{c} = \boldsymbol{M}(\phi, 0, 0)\boldsymbol{c}\boldsymbol{M}(\phi, 0, 0)^T$$

[7]Note, that some authors [53, p. 168] consider the difference $c_{11} - c_{12} - 2c_{44}$ instead of the ratio.

[8]In crystallography, x-, y and z-axis is often used as notation.

The resulting elastic matrix for a transversely isotropic crystal then becomes

$$\boldsymbol{c} = \begin{pmatrix} c_{11} & c_{12} & c_{13} & \cdot & \cdot & \cdot \\ & c_{11} & c_{13} & \cdot & \cdot & \cdot \\ & & c_{33} & \cdot & \cdot & \cdot \\ & & & c_{44} & \cdot & \cdot \\ & & & & c_{44} & \cdot \\ & & & & & c_{66} \end{pmatrix}_{(5)} , \qquad c_{66} = \frac{1}{2}(c_{11} - c_{12}) \tag{2.30}$$

It should be stressed that this matrix is for the z-axis as symmetry axis. A different result, although of the same form, is obtained if one of the other coordinate axes (or for that matter an arbitrary direction) is chosen as the axis of symmetry. It is seen that the matrix is based on five independent elastic constants, assuming no *a priori* dependence between these constants.

In chapter 6 it will be shown, that a cubic material used as weld metal may be considered transversely isotropic on a macroscopic level. This requires the averaging of (2.28) over all rotations ϕ around the x_3-axis using (2.22)

$$\bar{\boldsymbol{c}} = \frac{1}{2\pi}\int_0^{2\pi} \boldsymbol{M}(\phi,0,0)\boldsymbol{c}\boldsymbol{M}(\phi,0,0)^T \,\mathrm{d}\phi$$

This results in the following transversely isotropic elastic constants $\bar{c}_{ij}$ expressed in terms of the original cubic constants c_{ij}

$$\bar{c}_{11} = \bar{c}_{22} = \frac{1}{4}(3c_{11} + c_{12} + 2c_{44}) \tag{2.31a}$$

$$\bar{c}_{33} = c_{11} \tag{2.31b}$$

$$\bar{c}_{12} = \frac{1}{4}(c_{11} + 3c_{12} - 2c_{44}) \tag{2.31c}$$

$$\bar{c}_{13} = \bar{c}_{23} = c_{12} \tag{2.31d}$$

$$\bar{c}_{44} = \bar{c}_{55} = c_{44} \tag{2.31e}$$

$$\bar{c}_{66} = \frac{1}{4}(c_{11} - c_{12} + 2c_{44}) \tag{2.31f}$$

$$\bar{c}_{ij} = 0, \quad \text{else} \tag{2.31g}$$

As expected, the transverse isotropy condition $\bar{c}_{66} = \frac{1}{2}(\bar{c}_{11} - \bar{c}_{12})$ is satisfied, but furthermore, we have

$$\bar{c}_{12} - \bar{c}_{66} = \bar{c}_{13} - \bar{c}_{44} \tag{2.32}$$

That is, due to the inherited cubic symmetry, this form of transverse isotropy only has four independent elastic constants as opposed to five constants in general [53].

Table 2.3 lists the elastic properties of three transversely isotropic materials. The first material (X 6 CrNi 18 11) are directly measured constants [9, 53] (except c_{12} which has been calculated using the additional constraint in (2.30)), while the constants for the other two materials X 6 CrNi 18 12 and Inconel 182 have been obtained by applying (2.31) to the corresponding constants in Table 2.2. Concerning the directly measured constants for X 6 CrNi 18 11, the condition (2.32) is quite well met. The ratio between the lefthand side and the righthand side for this material is 96.5%.

An extensive analytic work on transversely isotropic crystals can be found in [62].

	Name	X 6 CrNi 18 11	X 6 CrNi 18 12	Inconel 182
ρ	$[10^3\text{kg/m}^3]$	7.82	7.90	8.61
c_{11}	$[10^{11}\frac{N}{m^2}]$	2.4110	2.63	2.78
c_{12}		0.96920	0.983	1.15
c_{13}		1.3803	1.45	1.3889
c_{33}		2.4012	2.16	2.5376
c_{44}		1.1229	1.29	1.06
c_{66}		0.7209	0.823	0.817

Table 2.3: Elastic properties for transversely isotropic materials.

2.5.4 Monoclinic crystal

We shall not be concerned with the monoclinic crystal itself in this thesis. However it provides a framework which the systems described above fit nicely into.

The monoclinic crystal has exactly one elastic symmetry plane, whose normal vector we take along the $\boldsymbol{e}_2$ axis. The elastic matrix, which has thirteen independent constants, then reads

$$\boldsymbol{c} = \begin{pmatrix} c_{11} & c_{12} & c_{13} & \cdot & c_{15} & \cdot \\ & c_{22} & c_{23} & \cdot & c_{25} & \cdot \\ & & c_{33} & \cdot & c_{35} & \cdot \\ & & & c_{44} & \cdot & c_{46} \\ & & & & c_{55} & \cdot \\ & & & & & c_{66} \end{pmatrix}_{(13)} \tag{2.33}$$

The systems described above are seen to be included in this class. This crystal system covers most of the materials found in practice.

The elastodynamic problem involving this crystal system may conveniently be split up into an antiplane problem and an inplane problem. With reference to the coordinate system in Fig. 2.2, the antiplane problem is defined by considering the deformation vector $\boldsymbol{u}(x_1, x_3, t) = (0, u_2(x_1, x_3, t), 0)$ whereas the inplane problem is defined by considering the deformation vector $\boldsymbol{u}(x_1, x_3, t) = (u_1(x_1, x_3, t), 0, u_3(x_1, x_3, t))$, both being independent of x_2. The elastodynamic equation in the antiplane problem then becomes

$$\rho\ddot{u}_2 = c_{66}u_{2,11} + 2c_{46}u_{2,13} + c_{44}u_{2,33} \tag{2.34}$$

The inplane problem becomes somewhat more complicated

$$\rho\partial_{tt}\begin{pmatrix} u_1 \\ u_3 \end{pmatrix} = \begin{pmatrix} D_{11} & D_{12} \\ D_{12} & D_{22} \end{pmatrix}\begin{pmatrix} u_1 \\ u_3 \end{pmatrix} \tag{2.35}$$

where

$$\begin{aligned} D_{11} &= c_{11}\partial^2_{x_1x_1} + c_{55}\partial^2_{x_3x_3} + 2c_{15}\partial^2_{x_1x_3} \\ D_{12} &= c_{15}\partial^2_{x_1x_1} + c_{35}\partial^2_{x_3x_3} + (c_{13} + c_{55})\partial^2_{x_1x_3} \\ D_{22} &= c_{55}\partial^2_{x_1x_1} + c_{33}\partial^2_{x_3x_3} + 2c_{35}\partial^2_{x_1x_3} \end{aligned}$$

As will be shown later, this splitting into an antiplane and an inplane problem is an important concept. In the antiplane problem, the wave propagates in the x_1x_3-plane with a displacement in the perpendicular $\boldsymbol{e}_2$ direction. This problem is therefore often denoted a *shear horizontal* (SH) problem.

The monoclinic elastic matrix is the most general matrix which allows an uncoupling between the antiplane and the inplane problem [49]. It is therefore often the point of departure in analytic modelling with problem formulation and results obtained for this system valid for the above described systems as well as a few other systems.

2.6 Review of existing modelling techniques

Today, numerous methods have been applied to the elastodynamic problems stated in the last section. At a higher level, these methods may be divided into either (purely) numerical approaches or analytical approaches. Achenbach [3] discusses some of the approaches.

In a numerical approach the whole problem is solved numerically through some sort of discretization technique such as the finite difference method (FDM) or finite element method (FEM). These approaches tend to be very versatile in their scope of applications, but due to their computer intensiveness they are in practice mainly restricted to 2D problems today. However, considering the speed with which CPU power and memory size increase, this approach will undoubtedly become more prominent. Still, another more fundamental aspect is the challenge of interpretation often associated with numerical solutions.

Analytical approaches, on the other hand, are rarely purely analytical. Often, only a formal analytical solution is derived. This solution must then be evaluated numerically. This is often the case when the solution is expressed in terms of an integral.

Analytical modelling of 2D and 3D problems is carried out at Department of Mechanics, Chalmers University of Technology, Göteborg, Sweden. This has resulted in several PhD theses [49,54,74] on the subject. In one of the activities, the whole NDT situation including the transmitter and receiver is modelled. The scenario is that of a homogeneous half-space with a transducer on the free surface (although the influence of a backwall also has been considered). Various types of smooth defects with orientation and geometry may be included in the half-space. The transducer is modelled by specifying the traction vector beneath it, thus the situation is as shown in Fig. 2.2 (with back- and sidewall approaching infinity). The method of solution as taken in [13] considering a penny-shaped defect is described roughly here for the sake of illustration. The sound field from the transducer is found by writing the displacement vector as an integral over plane monochromatic waves with arbitrary orientation (effectively a double Fourier transformation) and with coefficients specified so as to satisfy the boundary condition. If a pulse is modelled, the sound field from the transducer can then be written as a triple integral. The presence of the defect results in a scattered sound field. The incident sound field from the transducer as well as the scattered field are expanded in sums of spherical waves (involving Hankel functions and spherical harmonics) with the so-called transition (T) matrix (calculated using an integral equation method) specifying the linear relationship between the two sets of expansion coefficients, with the set for the incoming field being known. By using the *electromechanical reciprocity relations* [6] (these will also be studied later in the thesis), it is possible to model the transducer as a receiver thereby making it possible to obtain Ascans. The stationary phase approximation is used, making the obtained solution strictly valid only in the far field of the transducer. As the solution is found in the frequency domain, a desired pulse shape is also specified in this domain. A typical (symmetric) form is

$$\tilde{g}(f) = \begin{cases} \frac{1}{\Delta f}\cos^2\left(\frac{|f|-f_0}{2\Delta f}\pi\right), & f_0 - \Delta f < |f| < f_0 + \Delta f \\ 0, & \text{else} \end{cases} \tag{2.36}$$

where f_0 is the center frequency and Δf is the -6 dB bandwidth (half maximum width). Note that the support of the function is bounded and compact. This is a nice property concerning the (numerical) integration. An example is shown in Fig. 2.3 (left) for a center frequency $f_0 = 2\,\text{MHz}$ and bandwidths $\Delta f = 2\,\text{MHz}$ (solid line) and $\Delta f = 0.75\,\text{MHz}$ (dotted line). The inverse Fourier transform is simply

$$g(t) = -\frac{2\cos(2\pi f_0 t)\sin(2\pi\Delta f t)}{\Delta f t(4(\Delta f)^2 t^2 - 1)}$$

with the corresponding pulse shapes in the time domain shown in the right figure. As seen for the time domain the pulses are centered around $t = 0$ and with an in principle unbounded support. In this thesis, solutions are obtained directly in the time domain. Thus, the pulse shape in the time domain as in the right figure is actually of more interest here. However, for a given transducer, the pulse shape in both domains are usually given in the specifications.

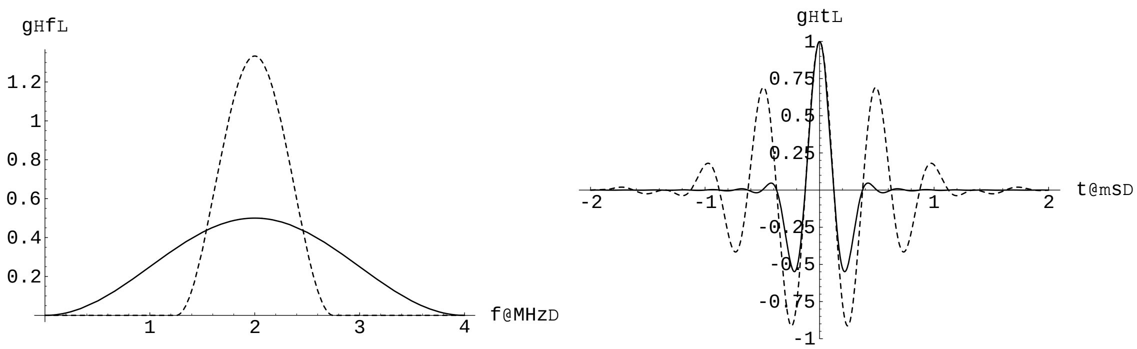

Figure 2.3: Pulse shapes in frequency domain (left) and time domain (right). Center frequency is $f_0 = 2\,\text{MHz}$ and bandwidths are $\Delta f = 2\,\text{MHz}$ (solid line) and $\Delta f = 0.75\,\text{MHz}$ (dotted line).

Originally, the above activity was restricted to isotropic media, but recently this activity has been extended to anisotropic media [49, 54] as well as anisotropic layered media [54], the last being an attempt to model laminated fiber composites and austenitic welds. Furthermore, it has now been possible to obtain the solution without the use of the stationary phase approximation, thus making the solution valid everywhere. Finally, an attempt of modelling scattering by rough cracks through perturbation methods has been carried out [37].

A number of these solutions has been collected into a command-line program UTDefect [12] running on a UNIX system, allowing the user to specify parameters for the specific

NDT situation as input. The program has been experimentally validated in [21]. In an attempt to facilitate the transition to industrial use, a windows-based PC version, named SUNDT[9], has been made. An evaluation copy of SUNDT (version 1.0) has been made available for free. An example of the windows-based presentation of results is shown in Fig. 2.4 with the above choice of pulse shape and parameters ($f_0 = 2\,\mathrm{MHz}$ and $\Delta f = 2\,\mathrm{MHz}$). A horizontal strip-like crack of width 5 mm and depth 30 mm is placed in steel. A 0° transducer is scanning a 20 mm×20 mm square directly above the crack in steps of 2mm in each direction (121 scanning positions). The user input is entered through a windows-based interface. The corresponding C-scan (mid bottom) is shown in the window indicating the horizontal crack edge. Different B-scans (left) may be chosen, and in each of these an A-scan (upper right) can likewise be chosen (here the amplitude is chosen to be relative to a side-drilled hole at the same depth). The required CPU time on a PII-450 was 2m15sec. Obviously, the required computer time is influenced by a number of factors, one of them being the number of scanning positions.

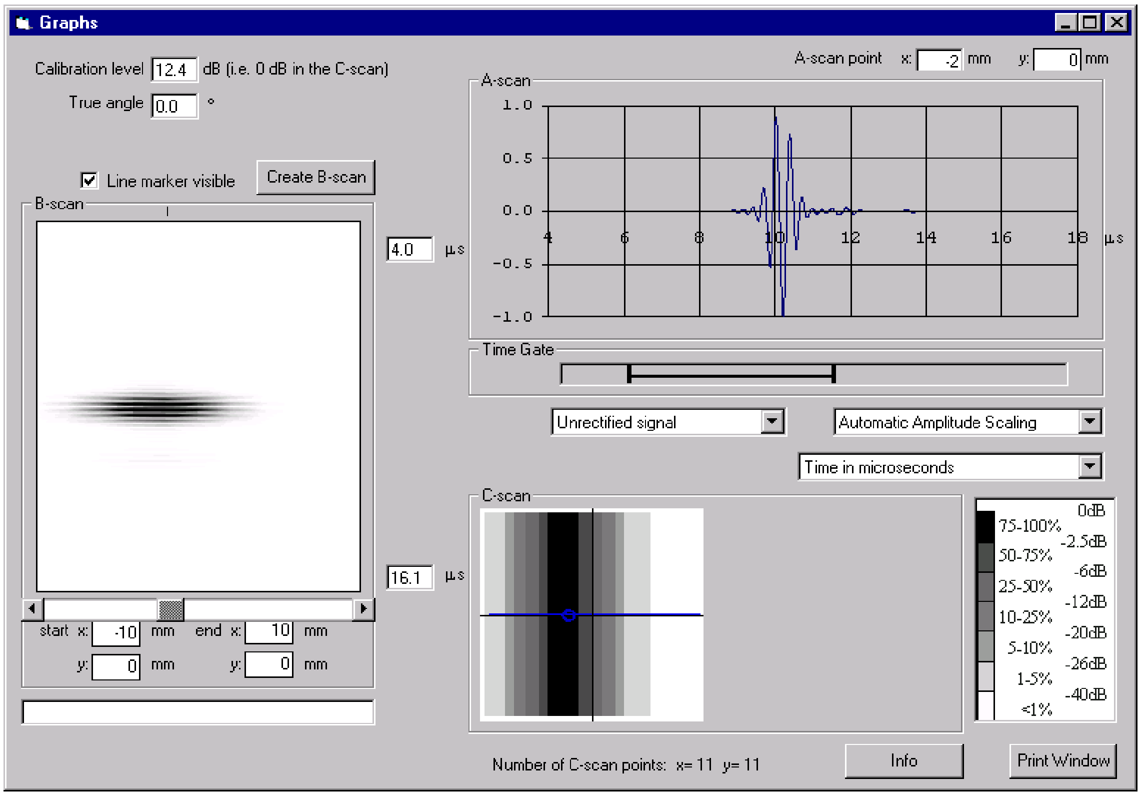

Figure 2.4: Example of the windows-based presentation of results in Sundt showing A-, B- and C-scans.

A different approach is that of ray tracing as described in [59]. In this approach, boundary conditions as well as transducer modelling are neglected. Only time-harmonic plane waves as solutions to the elastodynamic equations are considered. This approach was designed for simulation of the ultrasound path through anisotropic and inhomogeneous

[9]Copyright © SAQ Kontroll AB, Sweden.

materials such as an austenitic weld. The approach is based on the calculation of the energy vector associated with a plane wave with a given wave vector. These two vectors are parallel in the isotropic case, however, in the anisotropic case they are in general not parallel. The wave is then interpreted as following the direction of the energy vector. Plane waves and their characteristics will be described in more detail in the next chapter. Several papers exist [29,60,61] on this tool, known as RAYTRAIM, which is commercially available from AEA Technology. Other groups have also reported results using this approach [52,65]. The advantage of using this plane wave approach is a relatively short computation time and, being an analytic approach, the small amount of memory. Another advantage is the possibility of incorporating such a ray tracing code into a CAD program modelling complex geometries. This may provide the user with a first impression of the area being reached by the sound field. Such a model called UltraSim has been developed at FORCE Institute for isotropic, homogeneous materials. The drawback apart from not modelling the true sound field in the medium is that no A-scan information is provided.

Other analytic approaches to be mentioned here are those based on the Kirchhoff theory and Geometrical Theory of Diffraction (GTD). Both approaches are designed for studying the scattered field from smooth planar cracks in isotropic, homogeneous media. As will be seen, the two approaches may be regarded as being complementary to each other. According to Kirchhoff theory [3] (based on Huygen's principle), when considering a crack, the exact scattered field may be written as a surface integral over the crack of an integrand being the product of the displacement jump across the crack and a known Green's function for the material considered. However, as the jump in displacement across the crack is unknown this must be approximated by assuming that each point on the insonified surface reflects as though the crack was an infinite plane and the total field (sum of incident and scattered field) on the back (shadow) side of the crack is zero. With these assumptions the scattered field may then be found by evaluating the integral numerically. Due to the approximations made, the result is expected to be fairly accurate for cracks insonified close to normal incidence, where the scattered field is dominated by signals reflected off the crack surface. Geometrical theory of diffraction, first developed for optics [38] and later transferred to elastodynamics [4], states that two conical surfaces of diffracted rays (one of longitudinal and one of transverse nature) are generated when an incident ray strikes an edge. The half angles of the two conical surfaces to the edge tangent satisfy Snell's law. When approaching normal incidence, the two conical surfaces become discs. The diffraction coefficients relating the amplitude of the incident field to the two diffracted fields may be found analytically for isotropic materials in the high-frequency limit.

These two methods together with a transmitted probe beam model have been developed and implemented into a computer program to form a system model as described in [20], with the development and testing taking place at Nuclear Electric and AEA Technology. The main advantage of the two methods is the relatively simple nature of the model together with the small computation time as compared to a full analytic solution. The methods may also be found in stand-alone programs known as PEDGE (GTD) and PKIRCH (Kirchhoff theory). These have been developed by British Energy and AEA Technology in the 1980s. A model with the name MEPHISTO based on Kirchhoff theory has also been developed by the French Nuclear Energy Commision.

The section ends with a few remarks on numerical approaches. Application of the finite element method (FEM) to elastodynamic problems have been reported in [45, 46].

Here 2D and 3D problems are considered for isotropic as well as anisotropic materials. The echo from a strip-like crack is also considered. Reported computational times range from a few hours (2D) to seventy hours (3D). However, these are in 1990 CPU time. [51] uses a commercial code LS-DYNA2D to study ultrasonic NDT situations related to possible bonding defects in multi-layered structures within the aircraft industry. The Elastodynamic Finite Integration Technique (EFIT) will be studied in greater detail later in the thesis and will therefore not be discussed here. However, in the case of isotropic, homogeneous materials it reduces to the finite difference method (FDM) described in [69, 70]. These methods are characterized by considering both the time derivative of the displacement vector as well as the stress components (2.21) resulting in a set of coupled first order partial differential equations. The FDM method is used to study wave propagation in anisotropic, inhomogeneous media in [66]. In this approach the point of departure is the equation resulting from inserting (2.9) into (2.10), where now differentiation of the elastic matrix must be taken into account. Another approach is the application of the boundary element method (BEM) to the elastodynamic problem of a crack in an anisotropic medium as described in [73]. The main advantage of BEM over other numerical methods is the ability to obtain accurate numerical solutions at specified points in the material without having to carry out calculations over the whole domain.

Finally is mentioned the study of Gaussian wave packets in isotropic media using the method of characteristics in [56] and further developed in [55, 57] for anisotropic media.

2.7 Motivation of theoretical and numerical modelling

The elastodynamic problem has now been formulated in various ways (2.12), (2.13) and (2.21) with different existing approaches to these reviewed in the last section. It may generally be stated, that problems involving inhomogeneous materials are best solved using numerical methods, provided of course that sufficient knowledge about the inhomogeneity is available. The presence of anisotropy in the problem makes this statement only more true.

Due to the nature of the problem in this thesis, it has been decided to adopt the numerical method EFIT mentioned above. This method will be presented in detail in chapter 4.

However, valuable insight about the nature of solutions to elastodynamic problems may be provided from analytic activities. Qualitative insight is provided by studying plane waves as solutions to the elastodynamic equations. Qualitative as well as quantitative insight may be provided by studying the solution to a canonical problem such as the sound field from a load on the free surface of an elastic medium. The latter approach may furthermore be used to validate the numerical method. Thus, before concentrating on the numerical approach, chapter 3 will be devoted to the study of plane solutions as well as the solution to the problem of a line load situated at the free surface of an anisotropic, homogeneous medium.